Optics and Spectroscopy, 2022, Vol. 130, No. 2

16

Spectral optical properties of ceramic nanoporous membranes based on anodic aluminium oxide coated silver in ammonia vapors

© *M.Y. Vasilkov*[1,2¶], *I.N. Mikhailov*[1,2], *Y.V. Nikulin*[1,3], *S.S. Volchkov*[2], *D.A. Zimnyakov*[2], *N.M. Ushakov*[1,3]

[1] Saratov Branch, Kotel'nikov Institute of Radio Engineering and Electronics, Russian Academy of Sciences,
410019 Saratov, Russia
[2] Yuri Gagarin State Technical University of Saratov,
410008 Saratov, Russia
[3] National Research University n/a N.G. Chernyshevsky,
410012 Saratov, Russia
[¶] e-mail: vasilk.mikhail@yandex.ru

Received on April 29, 2021
Revised on June 22, 2021
Accepted on November 08, 2021

Spectral optical properties of synthesized ceramic nanoporous membranes based on anodic aluminum oxide coated silver in saturated ammonia gas flow have been experimentally investigated. Based on the measured transmission spectra and detected interference part of the spectra in wavelength range from 550 to 900 nm, temporal and spectral dependencies of the effective optical thickness and its changes in non-equilibrium conditions were obtained due to adsorption of ammonia molecules on silver film surface. According to detected and measured interference maximum shifts up to 14 nm in transmission spectra of $Al_2O_3 + Ag$ membranes in ammonia gas flow, the possibility of constructing a selective interferometric optical sensors with 10−15 min response time is shown.

Keywords: porous anodic aluminium oxide, membrane, silver film, light interference, ammonia vapors, effective optical thickness, interference maximum shift.

DOI: 10.21883/EOS.2022.02.53223.2244-21

Introduction

Porous anodic aluminum oxide (PAAO), obtained by a simple method of electrochemical anodization and characterized by a large specific surface area, high orderliness, and the ability to control structure parameters, has been attracting considerable attention in recent decades [1]. Porous films of anodic aluminum oxide (AAO) have been widely studied to create optical sensors on their basis based on the phenomena of fluorescence, surface enhanced Raman scattering of light (SERS) and surface plasmon resonance (SPR), as well as using reflection interferometric spectroscopy (RIfS) [2,3]. The method of reflection interferometric spectroscopy is based on reflection of white light from two boundaries of porous structures, which leads to amplification of the reflected light signal at wavelengths corresponding to the optical modes of the Fabry−Perot (FP) resonator formed by the thin film — environment system (Fabry−Perot effect) [4]. Adsorption of molecular particles on the pore surface causes a change in the refractive index in the structure and a shift in the wavelength of the interferometric bands, which can be detected and quantified [5]. Significant advantages of the nanoporous AAO platform compared to flat polymer films previously used for the RIfS method lie in provision of the unique three-dimensional morphology of pore structures, which makes it possible to modify it with various materials and create selective highly sensitive active surfaces for biomolecular and gas sensing applications [6]. The first articles on the use of the RIfS method using PAAO were devoted to the sensitive biomolecular detection of impurities in aqueous solutions [7,8], but its application to detect gas or vapor molecules was implemented only in the last decade [9,10]. It is assumed that shift of interference bands when interacting with gas molecules is caused by two phenomena: adsorption of gas on a porous surface and filling of pores due to capillary condensation [11]. Both of these effects can potentially be used to detect gas or vapor, depending on the physical and chemical properties of the detected molecules. However, most gases do not condense inside the pores. To detect these gases, it is necessary to achieve their binding to the PAAO surface. Strong adsorption of gas molecules at the PAAO/air interface can change the optical properties of the porous layer and cause a shift in the interference signal. To achieve this condition, it is necessary to sensitize the PAAO pore surface with thin metal films that have good affinity for adsorption of certain gas molecules and do not significantly affect the optical properties of the initial structure. To demonstrate this concept, two different metal films (Au and Pt) were deposited on PAAO in [9] and detection of hydrogen (H_2) and hydrogen sulfide (H_2S) using them was demonstrated. To confirm this concept, it is necessary to select a metal-gas pair with high affinity for adsorption of gas molecules on the metal surface. At the same time, the interference properties of PAAO membranes were studied in the equilibrium steady state regime of gas adsorption. It is also of interest to study the nonequilibrium interference properties of a PAAO membrane with different combinations of a metal film–gas

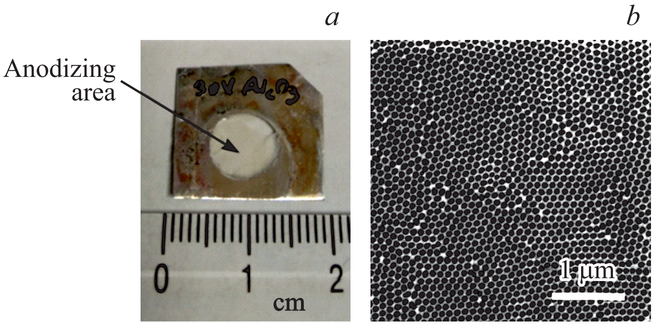

Figure 1. Appearance (*a*) and SEM micrograph of the surface of the PAAO (*b*) membrane obtained by anodizing in 0.3 M $H_2C_2O_4$ at temperature of 2−4°C and voltage of 30 V.

pair. One of such pairs, in our opinion, can be a thin film of silver and ammonia. It should be noted that a small number of articles on the study of ammonia sensors based on various physical (optical) principles have been published. There is a well-known article [12], in which sensor devices made of Fe_3O_4/MW-CNT-PhCOOH hybrid composites with different iron scale content were studied at low temperature, as well as some others [13,14].

The aim of this article is to experimentally study the dependence of the interference properties of a PAAO membrane coated with a thin silver film on the residence time in a dynamic ammonia gas flow.

Materials and methods

The initial material for obtaining the PAAO + Ag composite was aluminum foil (99.9%) with a thickness of $\sim 100\,\mu$m. Primary anodic oxidation of aluminum was carried out to prepare and structure the substrate surface in order to form an oriented system of porous channels. The process was carried out in 0.3 M solution of $H_2C_2O_4$ in an electrochemical cell made of inert material at temperature of 2−4°C in the two-electrode mode. A working sample made of aluminum was connected to the positive pole of the current source (anode), a perforated steel electrode of equal area — to the negative pole (cathode). A constant voltage in the range of (30 ± 1) V was applied to the electrodes, the distance between which was 10−15 mm, and maintained for 15−20 h. The thin Al_2O_3 layer obtained after primary anodization on the metal surface had a disordered porous structure („sacrificial layer“) and was removed by chemical etching at 85−90°C in aqueous solution of CrO_3 (puriss.) and H_3PO_4 (80%) with concentration of components of 20 g/l and 35 ml/l, respectively.

The metal prepared after chemical etching was subjected to second anodization for 1 h under conditions similar to primary anodic oxidation, as a result of which an ordered porous structure Al_2O_3 was formed on the surface of Al. To impart optical transparency to the PAAO sample, the metal sublayer was dissolved at room temperature in a mixture containing 45 ml/l HCl (38%) with addition of 67.5 g/l $CuCl_2$. As a result, thin PAAO membranes were obtained (Fig. 1, *a*), one side of which had an „open“ porous structure (Fig. 1, *b*), and the other was covered with a continuous layer of Al_2O_3. To form a matrix of hollow channels, a continuous oxide layer was dissolved in 5% solution of H_3PO_4 (80%). Thickness of the PAAO membrane, found by profilometry, did not exceed $4.0\,\mu$m. The average inner diameter of Al_2O_3 nanopores was (40.4 ± 3.6) nm with packing density of $1.8 \cdot 10^{10}\,\text{cm}^{-2}$.

Silver was deposited using DC magnetron sputtering with the following operating parameters: $U = 364$ V, $I = 100$ mA, $L = 60$ mm, $P_{\text{base}} \sim 4 \cdot 10^{-6}$ Torr, $P_{\text{Ar}} \sim 10^{-3}$ Torr, deposition rate Ag ~ 20 nm/min . The optimal sputtering time and thickness of the silver layer found in the course of preliminary experiments were 10 s and 3.6 nm, respectively.

The gas-sensitive properties of PAAO + Ag were studied on a measuring installation consisting of a chamber with a sample, a gas-mixing part and optical part. The diagram of the measuring installation optical part is shown in Fig. 2. The chamber for the sample was made of inert material (teflon) and was a sealed container with volume of ~ 500 ml, in the walls of which 4 holes were located perpendicular to each other in pairs for supplying and removing gas and radiation passing. The chamber contained a sample holder (CUV-UV cell holder, Ocean Optics), in which a flat PAAO + Ag sample was placed orthogonally to the radiation, and a gas flow was set along the sample surface. To ensure gas flow, an Omron NE-C28 electric gas compressor was used, which was connected by a constant flow of laboratory air through a triple valve to a high-speed Richter bubbler filled with a saturated aqueous ammonia solution (20°C). The gas mixture (air with saturated ammonia vapor) supply rate was controlled using a triple valve, one outlet of which was connected to a Richter bubbler, and the other outlet - to the atmosphere. By selecting a certain degree of opening the outlet to atmosphere, we achieved air bubbling through the Richter flask with a frequency of $\sim 100\,\text{min}^{-1}$, which corresponded to the rate of gas-air mixture supply of ~ 170 ml/min to the measuring chamber with the sample. The ammonia vapor concentration c(NH_3) in the supplied gas-air mixture was ~ 440 kppm, $p(NH_3) = 335.5$ mm Hg (20°C, 101.3 kPa, 25% aqueous solution of NH_3).

Spectral interference measurements of an optically transparent PAAO+Ag membrane were performed on an Ocean Optics QE65000B spectrometer with a DH-2000-BAL halogen-deuterium lamp (Ocean Optics) using the spectrasuite control program with an integration time of 100 ms. The spectral scan rate was 7.5 nm/ms. The interference spectroscopy method is based on light interaction with optical structures, in which reflected or transmitted light is amplified at certain wavelengths, creating characteristic interferometric spectra due to the Fabry-Perot effect. In PAAO + Ag, the Fabry-Perot effect can be described by the equation

$$EOT = 2n_{\text{eff}}L\cos\theta = m\lambda, \tag{1}$$

where EOT — effective optical thickness of the PAAO + Ag membrane, n_{eff} — effective refractive index, L — physical thickness of the membrane, m — order of interference bands, λ — light wavelength, θ — light incidence angle. For normal light incidence in our case $\cos\theta = 1$.

Expression (1) can be used to quantify changes in the optical properties of a membrane using changes in effective optical thickness ($DEOT$) as a measurement parameter [15]. The $DEOT$ value depends on the change in the membrane thickness due to adsorption of a molecular film on its surface and on the dependence of effective refractive index of the membrane on the incident light wavelength due to its dispersion:

$$DEOT(t,\lambda) = 2\cos\theta(\Delta d(t)n(\lambda) + d(t)\Delta n(\lambda)). \qquad (2)$$

If we assume that $\Delta d(t)n(\lambda) \ll d(t)\Delta n(\lambda)$, then the changes in the effective optical thickness $DEOT$ will be mainly determined by effective refractive index of the PAAO + Ag structure+molecular film of adsorbed gas.

As a characteristic of ammonia detection on the membrane surface, PAAO + Ag was estimated by $DEOT$ at a certain point in time and at selected wavelengths: 650, 750, 850 nm. The total exposure time of the PAAO+Ag membrane samples in the ammonia gas flow was 30 min. With a discrete time sampling of 0, 2, 4, 6, 8, 10, 30 min, the interferometric transmission spectra of the optically transparent PAAO + Ag membrane were measured. In this case, measurement time for a spectrum with width from 200 to 900 nm was significantly less than the sampling time interval. Assuming the smallness of optical absorption in the PAAO + Ag membrane, the transmission spectra $T(\lambda)$ can be easily transformed into the reflection spectra $R(\lambda)$, as $R(\lambda) = -1 - T(\lambda)$. The use of the fast Fourier transform (FFT) in processing of reflection spectra makes it possible to obtain information about adsorption processes at given time.

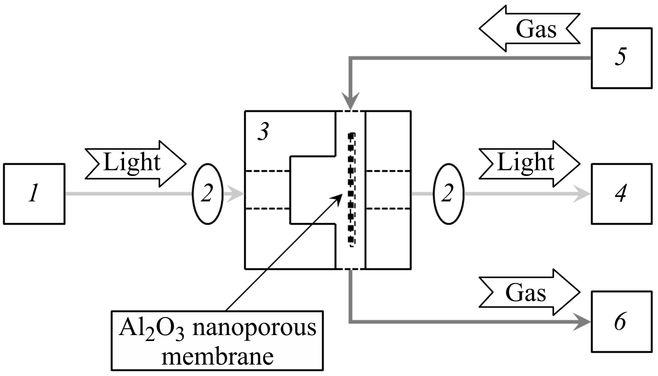

Figure 2. Diagram of a measuring bench for studying the optical characteristics of PAAO + Ag under influence of gas mixture with saturated ammonia vapor: *1* — radiation source (lamp), *2* — collimator, *3* — working chamber with PAAO + Ag sample (samples chamber), *4* — spectrometer, *5* — gas mixing part, *6* — release to atmosphere (in air). Light falls normally on the sample in the chamber.

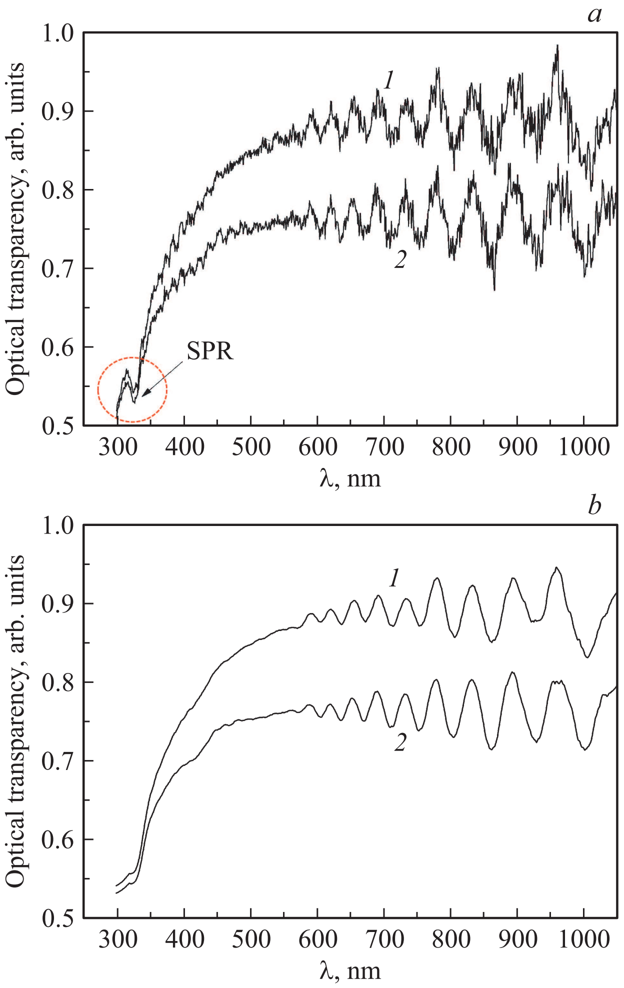

Figure 3. Transparency (transmission) spectra of PAAO + Ag measured in air and in the chamber before gas puffing (*a*) and the same spectra after treatment (*b*): measurement in air (*1*), measurement in the chamber at the moment of gas puffing (*2*).

Experimental results and discussion thereof

The dependences of the PAAO + Ag sample transmission were obtained in the range from 200 to 900 nm in air atmosphere and in the presence of saturated ammonia vapors. Figure 3, *a* shows the transmission spectra measured outside the chamber in air (curve *1*) and in the chamber before gas puffing (curve *2*). In the vicinity of the wavelength of 330 nm, a feature is noted — a local decrease in transmission (transparency) associated with manifestation of surface plasmon resonance (SPR) on a thin silver film ($d \sim 3.6$ nm). To reduce noisiness of the spectra, they were processed using the Origin 8 graphics package (Fig. 3, *b*). The decrease in the spectral transmission of the sample when it is located in the chamber is due to additional light reflection from the chamber entrance window. As can be seen, for all spectral lines in the wavelength range from 550 to 900 nm, light interference is clearly manifested.

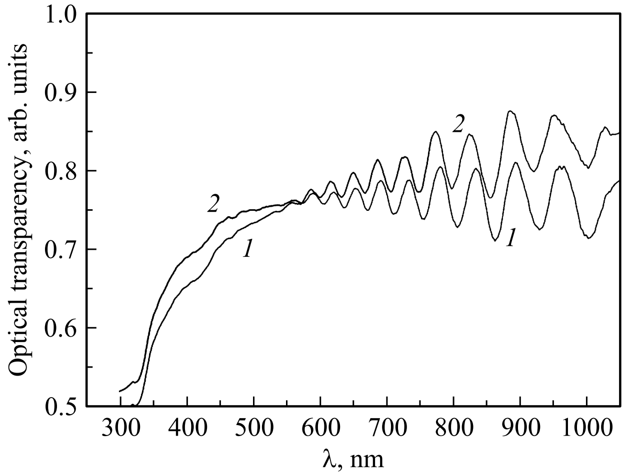

Figure 4. Transparency (transmission) spectra of PAAO–Ag for different time values of gas puffing into the measuring chamber: measurement in the chamber after 2 min (*1*), 30 min (it2).

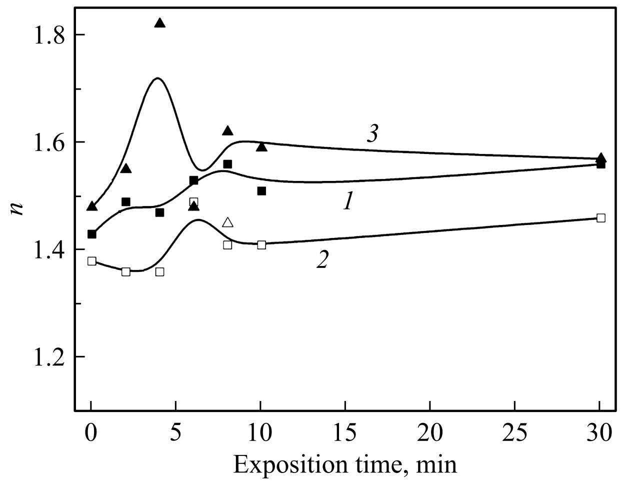

Figure 5. Dependences of the effective refractive index of the PAAO + Ag membrane on the time of gas puffing into the measuring chamber at wavelengths of 650 (*1*), 750 (*2*), 850 nm (*3*).

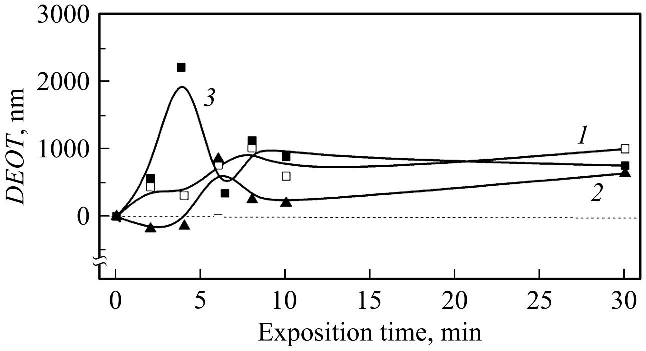

Figure 6. Dependences of the PAAO+Ag membrane effective optical thickness on the time of gas puffing into the measuring chamber at wavelengths of 650 (*1*), 750 (*2*), 850 nm (*3*).

When exposed to ammonia vapor, data were recorded every two minutes. As the exposure time increased, optical transparency of the PAAO + Ag membrane slightly increased, especially at long wavelengths. Figure 4 shows the optical transmission spectra measured after 2 min (curve *1*) and 30 min (curve *2*) of sample presence in the ammonia flow. An increase in sample transparency at long wavelengths is associated with an increase in optical impedance matching of the structure with incident electromagnetic waves.

Using the obtained interference pattern, it is easy to determine the refractive index of the membrane for the selected wavelength of the incident light. For two neighboring maxima of normally incident light, relation (1) can be represented as

$$2n_{\mathrm{eff}}L = m\lambda_1, \qquad 2n_{\mathrm{eff}}L = (m+1)\lambda_2. \tag{3}$$

From relation (3) it is easy to exclude the order of interference bands m and obtain the relation for the effective refractive index n_{eff}

$$n_{\mathrm{eff}} = \frac{\lambda_1\lambda_2}{2L(\lambda_2-\lambda_1)}. \tag{4}$$

Using relation (4) in the narrow spectral parts of the measured interference spectrum for three selected wavelengths (650, 750, 850 nm), the values of the membrane effective refractive index $n_{\mathrm{eff}}(\lambda)$ were determined. The obtained dependences of the PAAO + Ag membrane refractive index on the time of gas puffing into the measuring chamber are shown in Fig. 5. It should be noted the trend towards an increase in the refractive index for three wavelengths — 650, 750, 850 nm. The molecular film of adsorbed gas gradually grows with time, which is reflected in an increase in the effective refractive index at wavelengths of 650–850 nm.

A similar trend is manifested in the change in the effective thickness of the membrane. Figure 6 shows the $DEOT$ dependences of the PAAO + Ag membrane on the time of gas puffing into the measuring chamber at different wavelengths. As can be seen from the above dependences, the behavior of $DEOT$ is similar to the time dependences of the effective refractive index for different incident light wavelengths, which confirms correctness of the assumption for relation (2).

In support of the above, the FFT of the interference signals measured at different times at the previously selected wavelengths was carried out. An increase in the Fourier spectrum intensity for waves 650–850 nm indicates an increase in thickness of the molecular adsorbed layer of ammonia, while a decrease in the spectrum intensity indicates the processes of gas desorption on the silver surface. It should be noted that intensity of nonequilibrium adsorption and desorption processes is maximum within the time interval from 4 to 10 min.

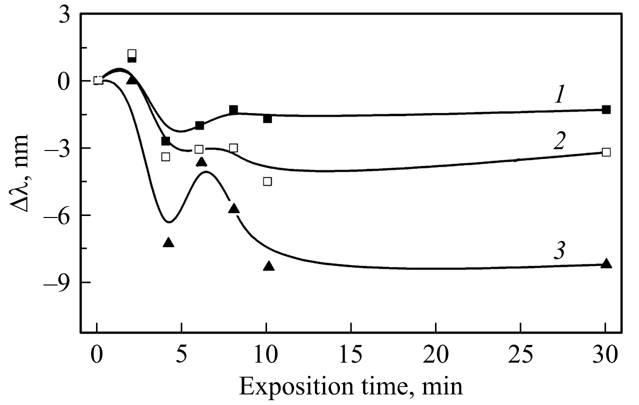

Figure 7. Spectral shift of the maximum (minimum) position depending on the time of gas puffing into the measuring chamber at wavelengths of 650 (*1*), 750 (*2*), 850 nm (*3*).

In the course of PAAO + Ag exposure to gas, a shift of interference maxima to the short-wavelength region (blue shift) by up to 14 nm is observed compared to the same value when exposed to air (Fig. 7). The shift value depends on the exposure time and practically does not change after 15 min exposure of the working sample in the gas flow. The time of 15 min, at which the maximum interference band shift is observed, can be attributed to the time of equilibration or the response time constant of the optical sensor based on the used material of PAAO + Ag.

The gas-sensitive properties of the resulting Ag/Al_2O_3-composite were tested with respect to saturated vapors of volatile organic substances (ethanol, acetone, isopropanol) in a mixture with air, however, a significant response was not received. A significant sensory response of the PAAO + Ag membrane was obtained with respect to saturated ammonia vapor and is explained by high selectivity of the synthesized material to this gas due to complex formation [16] and is confirmed by literature data [17,18].

Conclusion

The results of an experimental study of the change in the interference properties of an optically transparent PAAO membrane 4 mkm thick with through pores, coated with a thin (3.6 nm) tunnel-transparent silver film, depending on the residence time in a saturated gas flow of ammonia with a concentration of ∼ 440 kppm and rate of 170 ml/min are provided. Changes in the interference properties of the optically transparent PAAO + Ag+molecular film membrane structure were studied in the wavelength range from 550 to 900 nm. In this case, the membrane effective optical thickness, the values of which were estimated within 30 min with a discrete sampling of 2 min at conditionally selected wavelengths of 650, 750, 850 nm, was used as the main characteristic of such changes. Based on the measured transmission spectra, the time and spectral dependences of the refractive index and the change in the effective optical thickness were obtained. For the obtained dependences of the PAAO + Ag membrane refractive index on the time of gas puffing into the measuring chamber, a tendency to an increase in the refractive index for three wavelengths — 650, 750 and 850 nm should be noted. It has been shown by the transmission spectra FFT method that the intensity of nonequilibrium adsorption processes is maximum within the time interval from 4 to 10 min.

In the course of PAAO+Ag exposure to ammonia, a shift of interference maxima to the short-wavelength region (blue shift) by up to 14 nm is observed compared to the same value when exposed to air. The shift practically did not change after 10–15 min of working sample exposure in atmosphere with gas. Therefore, the time of 15 min can be estimated as the equilibration time or as the response time constant of the optical sensor based on the PAAO + Ag material used. It should be noted that when ammonia was replaced by volatile organic compounds (ethanol, acetone, isopropanol), no changes were detected in the interference part of the transmission spectrum, which indicates selectivity of ammonia adsorption on the PAAO + Ag surface.

Funding

The article was prepared within the scope of the state task „Sensor“ and with the financial support of the RFBR grants № 19-32-90221 and № 20-07-00968.

Conflict of interest

The authors declare that they have no conflict of interest.

References

[1] T. Kumeria, A. Santos, D. Losic. Sens., **14** (7), 11878 (2014). DOI: 10.3390/s140711878

[2] A. Yamaguchi, K. Hotta, N. Teramae. Anal. Chem., **81** (1), 105 (2009). DOI: 10.1021/ac8015642

[3] A.G. Koutsioubas, N. Spiliopoulos, D. Anastassopoulos, A.A. Vradis, G.D. Priftis. J. Appl. Phys., **103**, 094521 (2008). DOI: 10.1063/1.2924436

[4] V.S.Y. Lin, K. Motesharei, K.P.S. Dancil, M.J. Sailor, M.R. Ghadiri. Science, **278** (5339), 840 (1997). DOI: 10.1126/science.278.5339.840

[5] C. Pacholski, L.A. Perelman, M.S. VanNieuwenhze, M.J. Sailor. Phys. Stat. Sol. A, **206** (6), 1318 (2009). DOI: 10.1002/pssa.200881072

[6] F. Casanova, C.E. Chiang, A.M. Ruminski, M.J. Sailor, I.K. Schuller. Langmuir, **28** (17), 832 (2012). DOI: 10.1021/la204933m

[7] S. Pan, L.J. Rothberg. Nano Lett., **3** (6), 811 (2003). DOI: 10.1021/nl0340551

[8] S.D. Alvarez, C.-P. Li, C.E. Chiang, I.K. Schuller, M.J. Sailor. ACS Nano, **3** (10), 3301 (2003). DOI: 10.1021/nn900825q

[9] T. Kumeria, D. Losic. Phys. Stat. Sol. Rapid Res. Lett., **5** (10–11), 406 (2011). DOI: 10.1002/pssr.201105425

[10] S. Kaur, C.S. Law, N.H. Williamson, I.M. Kempson, A. Popat, T. Kumeria, A. Santos. Anal. Chem., **91** (8), 5011 (2019). DOI: 10.1021/acs.analchem.8b04963

[11] F. Casanova, C.E. Chiang, C.-P. Li, I.V. Roshchin, A.M. Ruminski, M.J. Sailor, I.K. Schuller. Nanotech., **19** (31), 315709 (2008). DOI: 10.1088/0957-4484/19/31/315709/

[12] A. Pistone, A. Piperno, D. Iannazzo. Sens. Actuators B, **186**, 333 (2013). DOI: 10.1016/j.snb.2013.06.027

[13] H.O. Ali. Transact. IMF, **95** (6), 290 (2017). DOI: 10.1080/00202967.2017.1358514

[14] T. Kumeria, A. Santos. Electrochemically Engineered Nanoporous Materials (Springer, Cham, 2015). p. 187–218. DOI: 10.1007/978-3-319-20346-1_7

[15] M. Nemati, A. Santos, T. Kumeria, D. Losic. Anal. Chem., **87** (17), 9016 (2015). DOI: 10.1021/acs.analchem.5b02225

[16] A.Yu. Olenin. Zhurnal neorg. khimii, **65** (4), 542 (2020) (in Russian). DOI: 10.31857/S0044457X20040157

[17] B. Wu, X. Zhang, B. Huang, Y. Zhao, C. Cheng, H. Chen. Sens., **17** (9), 2070 (2017). DOI: 10.3390/s17092070

[18] D. Kwak, Y. Lei, R. Maric. Talanta, **204**, 713 (2019). DOI: 10.1016/j.talanta.2019.06.034